Segmentation de scènes extérieures à partir d'ensembles d'étiquettes à granularité et sémantique variables

Damien Fourure, Rémi Emonet, Elisa Fromont, Damien Muselet, Alain Tremeau, Christian Wolf

Segmentation de scènes extérieures à partir d'ensembles d'étiquettes à granularité et sémantique variables

Fourure Damien[1]   Emonet Rémi[1]   Fromont Elisa[1]
Muselet Damien[1]   Tremeau Alain[1]   Wolf Christian[2]

[1] Univ Lyon, UJM, CNRS, Lab Hubert Curien UMR 5516, F-42000, SAINT-ETIENNE, France
[2] Université de Lyon, CNRS, France, INSA-Lyon, LIRIS, UMR5205, F-69621

Résumé

Ce papier présente une approche permettant d'utiliser plusieurs bases de données annotées avec différents ensembles d'étiquettes pour améliorer la précision d'un classifieur entrainé sur une tâche de segmentation sémantique de scènes extérieures. Dans ce contexte, la base de données KITTI nous fournit un cas d'utilisation particulièrement pertinent : des sous-ensembles distincts de cette base ont été annotés par plusieurs équipes en utilisant des étiquettes différentes pour chaque sous-ensemble. Notre méthode permet d'entraîner un réseau de neurones convolutionnel (CNN) en utilisant plusieurs bases de données avec des étiquettes possiblement incohérentes. Nous présentons une fonction de perte sélective pour entrainer ce réseau et plusieurs approches de fusion permettant d'exploiter les corrélations entre les différents ensembles d'étiquettes. Le réseau utilise ainsi toutes les données disponibles pour améliorer les performances de classification sur chaque ensemble. Les expériences faites sur les différents sous-ensembles de la base de données KITTI montrent comment chaque proposition contribue à améliorer le classifieur.

Mots Clef

Deep Learning, Réseaux de neurones de convolution, Segmentation sémantique.

Abstract

In this work, we present an approach that leverages multiple datasets annotated using different classes (different labelsets) to improve the classification accuracy on each individual dataset. We focus on semantic full scene labeling of outdoor scenes. To achieve our goal, we use the KITTI dataset as it illustrates very well the focus of our paper : it has been sparsely labeled by multiple research groups over the past few years but the semantics and the granularity of the labels differ from one set to another. We propose a method to train deep convolutional networks using multiple datasets with potentially inconsistent labelsets and a selective loss function to train it with all the available labeled data while being reliant to inconsistent labelings. Experiments done on all the KITTI dataset's labeled subsets show that our approach consistently improves the classification accuracy by exploiting the correlations across datasets both at the feature level and at the label level.

Keywords

Deep Learning, Convolutional neural network, semantic labelling, inconsistent labelling.

1   Introduction

Semantic scene parsing (a.k.a. semantic full scene labeling) from RGB images aims at segmenting an image into semantically meaningful regions, i.e. to provide a semantic class label for each pixel of an image — see Table 2 for examples of labels in an outdoor context. Semantic scene parsing is useful for a wide range of applications, for instance autonomous vehicles, automatic understanding and indexing of video databases, etc.

Most semantic scene parsing methods use supervised machine learning algorithms and thus rely on densely labeled (manually annotated) training sets which are very tedious to obtain. Only a small amount of training data is currently available for this task, which makes this problem stand out from other problems in vision (as for instance object recognition and localization). This is a particularly stringent problem for the currently most performing family of models in computer vision, namely deep networks, which are particularly needy in terms of training data. In the case of depth images, data-augmentation using artificially-created training data has been employed successfully for segmentation problems [1, 2]. However, the high variations of content in fully textured images make this solution at the moment very difficult to use for RGB images.

Most datasets for scene parsing contain only several hundreds of images, some of them only several dozen [3, 4, 5, 6, 7, 8, 9, 10, 11]. Combining these datasets is a non-trivial task as target classes are often tailored to a custom application. For example, one might be interested in specific types of vegetation like *trees*, *bushes* and *grass*, or types of objects such as *graffiti* or *billboard* while other applications do not require discriminating between these types. In this work, we present a solution to this problem by learning a

joint prediction model on a dataset composed of different and inconsistently labeled subsets.

The contributions of this paper are threefold : (i) we propose a deep network capable of processing features and labels (as input) from several different datasets and providing predictions for each of these datasets. Early layers are shared over datasets, whereas later layers are separated ; (ii) we show that shared parameters can lead to significant improvements of performance even if the semantic meanings of the different labelsets are different ; (iii) our experiments done on 7 annotated subsets of the KITTI dataset [12, 13] show that the label definitions, albeit inconsistent, are highly correlated, and that the proposed networks are able to capture and exploit these correlations.

2 Related Works

In this section, first, we discuss the state of the art on semantic scene parsing, then, we focus on feature and knowledge transfer methods, especially in the context of deep networks. Finally, we report several specific issues related to the KITTI benchmark which sparked wide interest and for which a limited range of methods has been proposed, especially in scene parsing.

2.1 Semantic Segmentation

Whereas the methods used for low level segmentation are diverse, high level semantic segmentation is dominated by machine learning, which can be explained by the high intra-class variances of this task. Learning methods range from random forests, to Support Vector Machines and deep networks. In [14] for instance, a structured-output version of random forests is proposed, where each leaf node predicts labels for every single pixel of an input patch, and predictions are integrated over patches using voting. Deep neural networks have also been used in wide range of works [15, 16, 17].

Over years, segmentation algorithms (semantic or not) have often been regularized through probabilistic graphical models like Markov Random Fields or Conditional Random Fields (CRF). Inference in these models requires to solve combinatorial problems which are often non-submodular and intractable. These methods have also been combined with machine learning, in particular deep networks [15]. Regrouping pixels into larger structures, like super-pixels, is also a frequently used technique [18, 15].

Auto-context models [19] are a different way to include structural information, which is computationally less expensive. They are defined by cascades of predictors, each one improving on the result of the previous. These models have also been adapted for scene parsing. In [16], similarly to recurrent networks for sequence classification, the same network is applied multiple times to outputs of different stages. In [17], a context learner is trained to predict context for a subsequent refinement learner. Both networks are trained on segmentation maps, but the refinement learner is trained to cope with noisy segmentations

as context input. In [20], scene parsing from depth images using auto-context is formulated as a graphical model and solved through message-passing.

Recent methods try to tackle the problem in a weakly supervised setting alleviating the problem on manual annotations [21, 22]. Instead of requiring pixelwise ground-truth, they integrate imagewise information, or pointwise groundtruth which can be easily provided. They are usually strongly regularized through priors like objectness [21] or classification performance based on the full image [22].

Segmentation methods specifically developed for the KITTI dataset are described in subsection 2.3.

2.2 Transferability

Lots of recent papers [23, 24, 25, 26, 27] proposed methods to solve the problem of the transferability of deep features. Since CNN require a lot of labeled data to provide very good features, the trend consists in exploiting features learned on one big dataset and in adapting them to other datasets and other tasks [26]. For example, in an extensive analysis about deep feature transfer, Yosinski et al. [26] show that it is better to transfer lower layers features learned on a different (and maybe distant) task than using random weights. These transfered features improve generalization performance even after fine-tuning on a new task. Hinton et al. [25] propose another way to transfer (or distill) knowledge from one big network to a small one. The idea is for the small network to learn both the outputs (soft targets) of the big network as well as the correct labels of the data. Accounting for the soft labels from the other network helps in learning the correlation between the labels. Furthermore, the authors showed that this distillation works well even when the transfer set that is used to train the final small model lacks any samples of one or more of the classes. When the dataset used to learn the first (source) network is different from the dataset used to fine-tune the final (target) network, it can be interesting to force the target and source features to be similar. This is the idea of Ganin and Lempitsky [23] who learn features that are invariant with respect to the shift between the source and target domains. Their solution consists in learning a domain classifier that tries to discriminate the two domains and to reverse the gradient during the backpropagation in order to learn features that cannot help in discriminating the domains. Very recently, Tzeng et al. [24] merge the two previous ideas (soft labels and domain confusion) into a framework that allows to transfer network knowledge across domains and tasks. Still in the context of domain adaptation, Zhang et al. [27] propose to match the source and target marginal distributions of features as well as the source and target conditional distributions of the labels associated to the features. Therefore, while learning the target network, they minimize both the marginal and conditional empirical Maximum Mean Discrepancy (MMD) between the source and target distributions. The domain adaptation problem is a bit different from our current problem, where we have a single dataset

partially labeled by different authors, with different and inconsistent labelings. Nevertheless, we can report three important points from the papers listed above : i) increasing the data helps generalization ; ii) fine-tuning for each specific task improves the classification and iii) exploiting the correlations between the labels also helps the classification. These observations guide the proposed approach.

2.3   The KITTI dataset

The KITTI Vision benchmark suite [12, 13] contains outdoor scene videos acquired on roads around the city of Karlsruhe, in rural areas and on highways. This very rich dataset was obtained using high-resolution color and grayscale video cameras in addition to depth information acquired using a Velodyne laser scanner and a GPS localization system. Many research teams work on this dataset since its release in 2013 tackling computer vision tasks such as visual odometry, 3D object detection and 3D tracking [5, 6, 7, 8, 9, 10, 11].

To tackle these tasks, several research teams have labeled some parts of the original video dataset, independently from the other teams, which means that some of the frames were labeled by more than one team, the ground truth segmentation quality varies, and the semantics and the granularity of the labels often differs. However, all the existing labels could be useful to tackle the scene labeling problem. Among the works listed, semantic segmentation is the final goal only for [7] and [11]. In [7] the authors jointly learn how to perform pixel classification and how to predict the depth of pixels. The depth classifier only predicts the likelihood of a pixel to be at any canonical depth (binary problem) and the join classifier is based on the multi-class boosted classifier suggested in [28]. In [11] the authors use a random forest (RF) classifier to classify segments of an image for different scales and sets of features (including depth information). Next they train another RF classifier on the segments with overlapping coverage to fuse, in a late fusion scheme, the unimodal classification results. Lastly they apply a CRF on the obtained results to enforce spacial consistency. None of the the 7 methods cited used deep learning to tackle the semantic segmentation step.

The aim of this paper is to show how to use inconsistent labeled in correlated data to improve the classification results. Meanwhile other papers use different features, such as color and depth, or color and temporal features, here we only use as input the simplest features available in KITTI : the RGB channels. Because of the use of different features (and of different tasks), that does not make sense to compare our classification accuracy results to the ones obtained for same individual subsets. They are however further discussed in the experiment part for sake of completeness.

3   Proposed Approach

Problem statement.   Given a set of images to label, which are drawn from a set of K different datasets, the pairs of input patches x_i^k and output labels y_i^k are grouped into sets $D_k = \{x_i^k, y_i^k\}$, where $k=1\ldots K$ and i indexes pixels. The label spaces are different over the different datasets, therefore each y_i^k can take values in space $\mathcal{L}^k$.

Our goal is to learn a nonlinear mapping $y = \theta(x, \Theta)$ with parameters Θ which minimizes a chosen risk $\mathcal{R}[\theta(x, \Theta){\neq}y]$. The mapping θ is represented as a convolutional neural network, where each layer itself is a nonlinear mapping $f_l(\mathbf{W}_l\mathbf{h}_{l-1} + \mathbf{b}_l)$ where $\mathbf{h}_l$ is the lth hidden representation, $\mathbf{W}_l$ and $\mathbf{b}_l$ are the weights and bias of the lth layer and $f_l(.)$ is the activation function of the lth layer.

We propose to minimize the empirical risk, then $\mathcal{R}[\theta(x, \Theta){\neq}y] = \frac{1}{N}\sum_{k=1}^{N} J(x, y, \Theta)$, where N is the number of training samples and J is the loss function for each individual sample. We also propose to use the cross entropy loss $J(x, y, \Theta) = -\sum_j 1_{y=j} \log \theta(x, \Theta)_j$, where $\theta(x, \Theta)_j$ is the network output for class j.

Limitations of separate training.   Considering K different datasets, the classical baseline approach is to train K separate mappings (models) θ^k, each defined on its own label set $\mathcal{L}^k$. Unfortunately this basic approach (illustrated in Figure 1a) presents several shortcomings :

(i) Each mapping θ^k is trained on its own dataset D^k, requiring a minimization over a separate sets of parameters Θ^k. In the chosen deep convolutional implementation the parameters $\Theta^k{=}\{\mathbf{W}^l, \mathbf{b}^l\}_{l=1}^{L}$ including all convolution filters and the weights of all fully connected layers, which are generally large sets (< 2 millions parameters). Learning such a large amount of parameters from limited (and generally small) amounts of training data is very challenging.

(ii) Relationships between label spaces are not modeled, which further limits the power of the trained models.

Joint feature training with selective loss.   We propose to tackle shortcoming (i) by exploiting the hierarchical nature of deep models. It is well known that, on most classical problems in computer vision, supervised training leads to a rising complexity of features over layers. Meanwhile early layers extract low level features, which exhibit strong independence of training input distribution and even task, later layers extract features which are more and more specific to the problem at hand [29].

We also propose to train a single deep network on the union of all individual datasets. Our network will share the parameters of its earlier layers for all datasets (to reduce overfitting), whereas the later layers will be duplicated for each dataset. This joint training approach is illustrated in Figure 1b. There is one output unit per label in the union of all label sets $\mathcal{L}^k$, which means that the output layer is able to provide predictions for each of the handled datasets. In a traditional multi-class setting involving a probabilistic loss function such as the cross-entropy, the network output o_j is computed using a soft-max function in the last layer. Classically, this can be seen as minimizing the negative log-likelihood (NLL) of the ground truth classes. However, with K different datasets, this choice is counter-productive as it also maximizes the NLL of all other classes, including classes that are not used in the training set. This will

FIGURE 1 – On top, the schema of the network used for our experiment. **(a)**,**(b)**,**(c)** and **(d)** show our different strategies. **(a)**, named *No Fusion* is our baseline and consists of learning one network per dataset. **(b)**, named *Joint training*, consists of learning only one network using all datasets with our selective loss function. **(c)** and **(d)**, respectively *Joint training with shared context* and *Joint training with individual context* add a Multi-Layer Perceptron at the output the network **(b)** (already learned) and fine tune it. The objective is that the added MLP takes into account the correlation between labels learned by **(b)**. The difference between **(c)** and **(d)** is that **(c)** learns all dataset simultaneously likewise the *Joint training* strategy when **(d)** fine tunes the networks with only one dataset.

lead to problems when there exists a correlation between labels across different datasets. As concrete example, in the KITTI dataset (see Table 2 where all labels are reported) the class *Tree* of the dataset from He et al. [5] is likely to be correlated with the class *Vegetation* from the dataset labeled by Kundu et al [6]. In our model, the normalization of the output probabilities is achieved using a dataset-wise soft-max : for each label j from dataset k,

$$f(j, \theta(x, \Theta)) = \frac{e^{\theta(x, \Theta)_j}}{\sum\limits_{j' \in \mathcal{L}^k} e^{\theta(x, \Theta)_{j'}}} \quad (1)$$

In practice, the datasetwise soft-max is combined with a selective cross-entropy loss function as follows :

$$J'(k, x, y, \Theta) = -\theta(x, \Theta)_y + \log(\sum\limits_{j \in \mathcal{L}^k} e^{\theta(x, \Theta)_j}) \quad (2)$$

Gradients are null for parameters involving output units corresponding to labels from datasets l with $l \neq k$. This is equivalent to using separate output layers for each dataset and intermediate layers with shared parameters over the different datasets.

Modeling correlations between labelsets. Shortcoming (ii) is partly addressed by the joint feature training, as correlations between labels across datasets can be learned by the shared layers in the network. On the other hand, we will show that explicitly modeling these correlations further improves the discriminative power of the classifier. To take into account the correlation between labelsets, we concatenate the outputs of the different networks $\theta^k(x, \Theta)$. We then feed the concatenation into a dataset-wise log-soft-max (see Eq. 1) followed by some additional

Authors	Train	Validation	Test	Total
He et al. [5]	32	7	12	51
Kundu et al. [6]	28	7	12	50
Ladicky et al. [7]	24	6	30	60
Ros et al. [8]	80	20	46	146
Sengupta et al. [9]	36	9	25	70
Xu et al. [10]	56	14	37	107
Zhang et al. [11]	112	28	112	252
Total	368	91	277	736

TABLE 1 – Number of images from the original KITTI dataset annotated by different research teams over the past 2 years. When available, we use the train/test split proposed in the corresponding publication.

fully-connected layers. After pre-training each individual $\theta^k(x, \Theta)$, new mappings $\theta'^k(x, \Theta)$ are trained, where each θ'^k combines the inputs from all $\theta^k, k = \{1 \ldots K\}$. In an end-to-end training setting, parameters of the full model are trained jointly (see Figure 1d).

We do not try to estimate from which dataset an input sample actually originated. Unlike transfer learning tasks, no shift is supposed in the input distributions of the different datasets, the difference being in the ground truth labels. Existing shifts in the input distributions can still be learned by the network, however.

4 Experimental Results

4.1 Training details

All experiments are done with the Torch7 [30] framework and training was operated on consumer GPUs. We used a
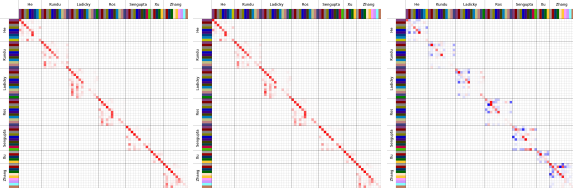
FIGURE 2 – Row-normalized confusion matrices for the *No Fusion* (left) and for the *Joint training with individual context* (center) learning strategies. The last matrix (right) highlights the differences between the two confusion matrices : blue (resp. blue) cells are for value that decrease (resp. increase) with *joint training* ; the darker the color the higher the variation. The 68 rows/columns correspond to the 68 labels shown in Table 2.

network architecture inspired by Farabet et al.[15] for outdoor scene labeling and improved with the recent advances in deep neural network research. Our network is composed by 3 convolutional layers followed by 2 fully-connected linear layers. The network is illustrated in Figure 1. The first two convolutional layers are composed by a bank of 7×7 filters followed by ReLU [31] units, 2×2 maximum pooling and batch normalization [32] units. The last convolutional layer is a simple filter bank followed by a ReLU unit, a batch normalization unit and dropout [33] with a drop factor of 30%. The first fully connected linear layer is then followed by a ReLU unit and the last layer is followed by our datasetwise softmax unit. We used this network to the our approach to obtain the results shown in lines 3 and 4 of Table 3 (illustrated in Figure 1c and 1d). Additional fully connected layers are added followed by a ReLU unit (and the datasetwise softmax unit for the output layer) and batch normalization units. To train the network, RGB images are transformed into YUV space. A training input example is composed of a patch x_i of size 46×46 cropped from the original image and centered around a pixel i, the dataset k from which the example comes from, and the label y_i^k corresponding to pixel i. Stochastic gradient descent with a mini-batch of size 128 was used to update the parameters. We used early stopping on a validation set in order to stop the training step before overfitting.

4.2 Dataset details

In addition to the information provided in Section 2.3 about the KITTI dataset, we now provide precise information about the labeled data. This is summarized in Table 1. The dataset has been partially labeled by seven research groups resulting in 736 labeled images that are split into : a train set, a validation set and a test set. When the information was given by the author, we used the same train/test set as them. Note that Xu et al. [10] provide a complete hierarchy of very detailed labels, but we only used the highest level of the hierarchy to obtain a labeling more compatible (in terms of granularity) with the labels from the other research teams. Also note that the KITTI dataset contains

over 40000 frames (180GB of raw videos) but in this work we only rely on the labeled data. We then sample on average 390.000 patches in each video frame (depending on its size). This results into a dataset of about 280 million patches suitable to train a deep learning architecture.

As mentioned in Section 2.3, the different labels provided by the different teams are not always consistent. As illustrated in Table 2, we can see that the granularity and the semantics of the labels may be very different from one labeling to another. For example, Ladicky et al. separate the *Trees* from the *Grass*. However, this might correspond to the *Vegetation* labels in the subset from Xu et al. but might also correspond (in the case of *Grass*) to the labels *Ground*. He et al. [5] have not used the labels *Pole*, *Sign* or *Fence* used in most other labelings. These labels are likely to overlap with the label *Building* of He et al. but then, this *Building* class cannot be consistent anymore with the other labelings that contain the label *Building* in other subsets. Some groups have used the label *Bike* and some others have used the label *Cyclist*. Those two labels are likely to overlap but in one case a team has focused on the entire entity "cyclist on a bike" whereas another has only focused on the bike device. These inconsistencies made the KITTI dataset a good candidate to test the proposed method.

4.3 Joint training

Table 3 shows the accuracy obtained for all our training strategies. We report the *global accuracy* and the *average accuracy*. *Global* is the number of correctly classified pixels over the total number of pixels (also called *recall* or *pixel accuracy*) and the *Average* is the average of this recall per class (also called the *class accuracy*). Note that the last column (*Total*) of the Table 3 gives the global and average accuracies for all sub datasets together so that the totals take into account the relative number of labeled pixels in each sub-dataset instead of being the average of all elements in the line.

The first learning strategy implemented consists in learning one network per dataset with the architecture described in Section 4 and illustrated in Figure 1.a. This is our baseline. The results for this strategy are shown in the first line (*No Fusion*) of Table 3. Note that the state-of-the-art results for each of those sub datasets are (respectively for global and average accuracies) : $(92.77, 68.65)$ for He et al. [5] ; $(97.20,$ non reported) for Kundu et al. [6] ; $(82.4, 72.2)$ for Ladicky et. al. [7] ; $(51.2, 61.6)$ for Ros et al. [8] ; $(90.9, 92.10)$ for Sengupta et al. [9] ; (non reported, 61.6) for Xu et al. [10] ; and $(89.3, 65.4)$ for Zhang et al. [11]. These results are often much better (except for Ros et al.) than those reported in Table 3. This can be obviously explained by the fact that : [6, 9, 7, 8] only show results computed from a subset of their labels (e.g. the label *pedestrian* is ignored in [9, 7, 8]) ; the features used by all methods are richer (e.g. depth and time) as discussed in Section 2.3 ; and the proposed methods always combine multiple classifiers tuned on one particular sub-dataset.

He et al.	Road	Building	Sky	Tree	Sidewalk	Car	Pedestrian	Bicyclist				VegetationMisc
Kundu et al.	Road	Building	Sky	Vegetation	Sidewalk	Car	Pedestrian	Cyclist	Pole	Sign	Fence	
Ladicky et al.	Road	Building	Sky	Tree	Sidewalk	Car	Pedestrian	Bike	Column	Sign	Fence	Grass
Ros et al.	Road	Building	Sky	Vegetation	Sidewalk	Car	Pedestrian	Cyclist	Pole	Sign	Fence	
Sengupta et al.	Road	Building	Sky	Veg.	Pavement	Car	Pedestrian		Poles	Signage	Fence	
Xu et al.	Ground	Infrastructure	Sky	Vegetation		Movable						
Zhang et al.	Road	Building	Sky	Vegetation	Sidewalk	Car	Pedestrian	Cyclist		Signage	Fence	

TABLE 2 – The 68 labels (with the original colors) used by the different authors to annotate their subset of the KITTI benchmark.
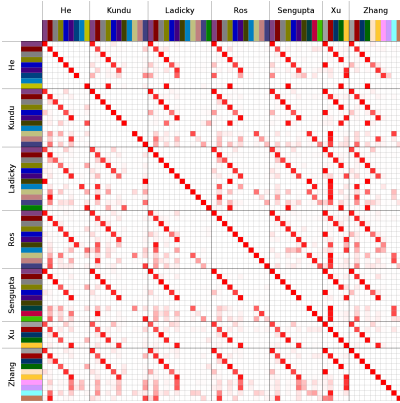
FIGURE 3 – Empirical Label correlation matrix. Each line corresponds to the average of the class probabilities predicted by the network for a given target class (among the 68 labels given in Table 2). Darker cells indicate higher probabilities. Non-diagonal red cells correspond to labels highly correlated with the target (main diagonal) label. Some entries (rows) have a no value due to the absence of example in the test set.

The second alternative strategy (*Joint Training*) consists in learning one single network (illustrated in Figure 1b) with all the datasets using the selective loss function detailed in Section 3. The second line of Table 3 shows that this strategy gives better results than our baseline (in total +1.81 for the pixel accuracy and +3.85 for the class accuracy). This result was expected since the amount of data used clearly increases from the *No Fusion* network (with a maximum of 112 training images for the subset labeled by Zhang et al.) to the *Joint training* strategy which uses 368 training images. This data augmentation leads to a better generalization and so to better classification accuracies. These results show that the selective loss function allows to successfully take into account the inconsistent labels.

4.4 Correlation rates between labelsets

When the *Joint training* network is trained, the correlation rates between labels of each sub dataset can be computed from the output probability vector of the datasetwise softmax units. We computed a label correlation matrix, shown in Figure 3, by averaging the predictions made by the network for each target class label (from one of the 7 possible labelings). The (full) diagonal of the matrix gives the correlation rates between the expected target labels. In each line,

the other non-zero values correspond to the labels correlated with the target label y_i^k. Please note that this is different from a confusion matrix since each line shows the average of the output probabilities and not the predictions. We can also see that a diagonal is visible in each block of the matrix (corresponding to the correlations between two different labelings) for the first 5 labels of each dataset. This means that, as expected, these first 5 labels are all correlated (for example, the label *Road* from He et al. is correlated with the label *Road* from Kundu et al. with the *Road* from Ladicky et al. etc.). A second observation is that the correlation matrix is not symmetric. For example, the classes *Building*, *Poles*, *Signage* and *Fence* from Sengupta et al. have (as already discussed in Section 4.2) a high correlation with the class *Infrastructure* from Xu et al., meaning that these classes overlap. On the contrary, the class *Infrastructure* from Xu et al. has a very high correlation with the class *Building* from Sengupta et al. and a limited one with the classes *Poles*, *Signage* and *Fence*. This is due to the target distributions. The *Building* class from Sengupta et al. is more represented than the three other classes so *Infrastructure* from Xu et al. is more correlated to *Building*. If these observations mostly confirm the expectations we discussed in Section 4.2, they show that our method can also be used to automatically discover correlations between labels.

4.5 Improvement from correlation modeling

The correlations studied in Section 4.4 not only help us to retrieve the hierarchical dependencies between all the labels but it can also improve the prediction accuracies. Using our method, the network can correct possible errors if another prediction correlated to the target one is more confident. These correlations are taken into account by adding a Multi-Layer Perceptron (MLP) after the output of the original network and by fine tuning the entire network with this added MLP.

The *Joint training with shared context* strategy, illustrated in 1c, consists in learning all datasets together with our selective loss-function (as for the *Joint training*). This third approach improves pixel accuracy (global) but not class accuracy (average), compared to *Joint training* (see Table 3 line 3 vs line 2). As the stochastic gradient descent optimizes the pixel accuracy (*global*) this leads to an overfitting. Indeed, an increase in *global*, together with a decrease in *average* can be a sign that the network starts to overspecialize : it strongly learns the distribution of classes to the detriment of learning the appearance of each class.

Results with all classes available in the ground truth										
		He	Kundu	Ladicky	Ros	Sengupta	Xu	Zhang	Total	
No Fusion	Global	74.67	72.48	72.94	76.96	78.71	86.97	84.98	80.94	-
	Average	58.56	56.04	43.16	48.76	71.26	83.11	57.39	57.14	-
Joint training	Global	78.68	77.20	75.86	78.22	81.48	88.02	86.89	82.75	(+1.81)
	Average	**64.41**	**60.61**	46.52	52.06	75.64	**85.14**	**60.54**	60.99	(+3.85)
Joint training with shared context	Global	78.61	**77.76**	76.00	78.40	**81.97**	**88.43**	**87.54**	83.16	(+2.22)
	Average	62.87	59.13	45.22	51.16	75.55	84.94	59.75	60.03	(+2.89)
Joint training with individual context	Global	**79.31**	77.53	**76.81**	**78.41**	80.98	88.35	86.76	**83.19**	(+2.25)
	Average	64.15	59.77	**47.92**	**52.35**	**77.19**	85.09	59.84	**61.24**	(+4.10)

TABLE 3 – Pixel (*Global*) and Class (*Average*) accuracy results for the 7 used sub-datasets with 4 different training strategies : NF=No Fusion (see Fig. 1a) ; JT= Joint training (see Fig. 1b) ; JTSC=Joint training with shared context (see Fig. 1c) ; JTIC=Joint training with individual context (see Fig. 1d). Best results are highlighted in bold.
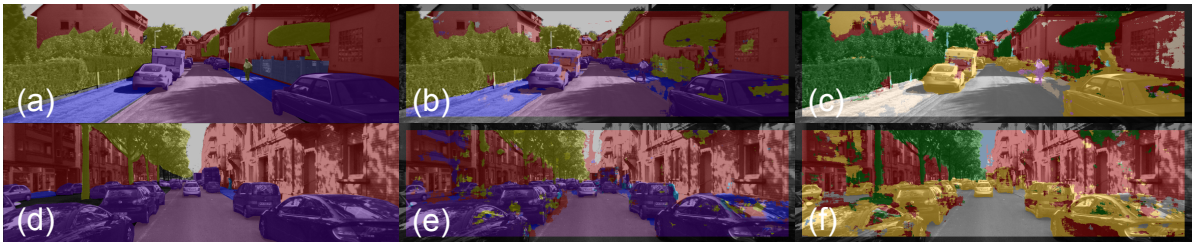

FIGURE 4 – Example of pixel classification results given by the JTIC strategy (see Figure 3). **(a)** is the ground truth from the Ros et al. labelset. **(b)** is the result obtained with our strategy for the same labelset and **(c)** is the result obtained for the Kundu et al. labelset. **(d)** is a ground truth image from He et al.. **(e)** is the result obtained for the same labelset and **(f)** is the result obtained for the Xu et al. labelset.

The *Joint training with individual context* (JTIC), illustrated in 1d, is based on the same approach as the Joint Training (JT) with shared context, but instead of learning all datasets together with the selective loss function the datasets are here learned one by one (by fine-tuning one network per dataset). The shortcoming of the JT approach is that when all datasets are learned together the features are general. By fine-tuning with only one dataset, we specialized the features for this datasets. The results from Table 3 line 4 show that in average this approach outperforms the other ones. Both the global and the average measures increase compared to *Joint training*, suggesting that this approach is more robust that the *Joint training with shared context*.

The confusion matrices computed from our baseline strategy next from the JTIC are shown in Figure 2. In order to better visualize the improvement, the matrix on the right shows the difference between the JTIC confusion matrix and the baseline one. Negative values are displayed in blue and positive values in red. As expected the majority of non-diagonal values are negative while the diagonal values are positive. This demonstrates that errors (non-diagonal) made by the first network were reduced by better (i.e. correct) predictions (diagonal) with JTIC. Looking more into the details, we can see what errors are corrected by JTIC. In most datasets, an important amount of *cars* were labeled as *buildings* by the baseline, meanwhile now they are pro-

perly labeled with our JTIC approach. To a lesser extent, the same is also observed for *sidewalks* and *grounds*.

5 Conclusion

This paper proposed and evaluated different strategies to take into account inconsistent labels in correlated data to improve outdoor full scene labeling. The proposed methods have been applied to the particular case of the KITTI dataset using only the RGB color features and labeled data of this dataset. To tackle the full scene labeling problem, one could rely on much more detailed features such as depth information, temporal information and the huge amount of unlabeled data available for this dataset. This constitute our future work. The main contribution of this paper is to propose a *Joint training with individual context* approach that allows to : leverage multiple datasets annotated using different classes (different labelsets) ; and improve the accuracy of the classification on each individual dataset. Experimental results show a clear improvement in terms of classification accuracy when multiple datasets are fused and further improvement when the last layers of the network are computed datasetwise.

Acknowledgment

Références

[1] J. Shotton, A. Fitzgibbon, M. Cook, T. Sharp, M. Finocchio, R. Moore, A. Kipman, and A. Blake, "Real-time human pose recognition in parts from single depth images," in *CVPR*, 2011. 1

[2] D. Tang, T. Yu, and T.-K. Kim, "Real-time articulated hand pose estimation using semi-supervised transductive regression forests," in *ICCV*, 2013. 1

[3] S. Gould, R. Fulton, and D. Koller, "Decomposing a scene into geometric and semantically consistent regions," in *ICCV*, 2009. 1

[4] C. Liu, J. Yuen, and A. Torralba, "Nonparametric scene parsing via label transfer," *IEEE TPAMI*, vol. 33, no. 12, 2011. 1

[5] H. He and B. Upcroft, "Nonparametric semantic segmentation for 3d street scenes," in *Intelligent Robots and Systems (IROS)*, 2013. 1, 3, 4, 5

[6] A. Kundu, Y. Li, F. Dellaert, F. Li, and J. M. Rehg, "Joint semantic segmentation and 3d reconstruction from monocular video," in *ECCV*, 2014. 1, 3, 4, 5

[7] L. Ladicky, J. Shi, and M. Pollefeys, "Pulling things out of perspective," in *CVPR*, 2014. 1, 3, 4, 5

[8] G. Ros, S. Ramos, M. Granados, A. Bakhtiary, D. Vazquez, and A. M. Lopez, "Vision-based offline-online perception paradigm for autonomous driving," in *Winter Conference on Applications of Computer Vision (WACV)*, 2015. 1, 3, 4, 5

[9] S. Sengupta, E. Greveson, A. Shahrokni, and P. H. Torr, "Urban 3d semantic modelling using stereo vision," in *IEEE ICRA*, 2013. 1, 3, 4, 5

[10] P. Xu, F. Davoine, J.-B. Bordes, H. Zhao, and T. Denoeux, "Information fusion on oversegmented images : An application for urban scene understanding," in *IAPR MVA*, 2013. 1, 3, 4, 5

[11] R. Zhang, S. A. Candra, K. Vetter, and A. Zakhor, "Sensor fusion for semantic segmentation of urban scenes," in *IEEE ICRA*, 2015. 1, 3, 4, 5

[12] J. Fritsch, J. T. Kuhnl, and A. Geiger, "A new performance measure and evaluation benchmark for road detection algorithms," in *Intelligent Transportation Systems-(ITSC)*, 2013. 2, 3

[13] A. Geiger, P. Lenz, C. Stiller, and R. Urtasun, "Vision meets robotics : The kitti dataset," *The International Journal of Robotics Research*, 2013. 2, 3

[14] P. Kontschieder, S. Bulo, M. Pelillo, and H. Bischof, "Structured labels in random forests for semantic labelling and object detection," *ICCV*, 2011. 2

[15] C. Farabet, C. Couprie, L. Najman, and Y. LeCun, "Learning hierarchical features for scene labeling," *IEEE TPAMI*, vol. 35, no. 8, 2013. 2, 5

[16] P. Pinheiro and R. Collobert, "Recurrent convolutional neural networks for scene labeling," in *ICML*, 2014. 2

[17] E. Fromont, R. Emonet, T. Kekec, A. Trémeau, and C. Wolf, "Contextually constrained deep networks for scene labeling," in *BMVC*, 2014. 2

[18] J. Tighe and S. Lazebnik, "Superparsing : Scalable nonparametric image parsing with superpixels," in *ECCV*, 2010. 2

[19] Z. Tu and X. Bai, "Auto-context and its application to high-level vision tasks and 3d brain image segmentation," *IEEE TPAMI*, vol. 32, no. 10, 2010. 2

[20] R. Shapovalov, D. Vetrov, and P. Kohli, "Spatial inference machines," in *CVPR*, 2013. 2

[21] A. Bearman, O. Russakovsky, V. Ferrari, and L. Fei-Fei, "What's the point : Semantic segmentation with point supervision," *arXiv :1506.02106*, 2015. 2

[22] P. Pinheiro and R. Collobert, "From image-level to pixel-level labeling with convolutional networks," in *CVPR*, 2015. 2

[23] Y. Ganin and V. Lempitsky, "Unsupervised domain adaptation by backpropagation," in *ICML*, 2015. 2

[24] E. Tzeng, J. Hoffman, T. Darrell, and K. Saenko, "Simultaneous deep transfer across domains and tasks," *arXiv*, vol. abs/1510.02192, 2015. 2

[25] G. Hinton, O. Vinyals, and J. Dean, "Distilling the knowledge in a neural network," in *NIPS Deep Learning Workshop*, 2014. 2

[26] J. Yosinski, J. Clune, Y. Bengio, and H. Lipson, "How transferable are features in deep neural networks ?," in *NIPS*, 2014. 2

[27] X. Zhang, F. X. Yu, S. Chang, and S. Wang, "Deep transfer network : Unsupervised domain adaptation," *arXiv*, vol. abs/1503.00591, 2015. 2

[28] A. Torralba, K. P. Murphy, and W. T. Freeman, "Sharing features : Efficient boosting procedures for multiclass object detection," in *CVPR (2)*, 2004. 3

[29] M. Zeiler and R. Fergus, "Visualizing and understanding convolutional networks," in *ECCV*, 2014. 3

[30] R. Collobert, K. Kavukcuoglu, and C. Farabet, "Torch7 : A matlab-like environment for machine learning," in *BigLearn, NIPS Workshop*, 2011. 4

[31] A. Krizhevsky, I. Sutskever, and G. Hinton, "Imagenet classification with deep convolutional neural networks," in *NIPS*, 2012. 5

[32] S. Ioffe and C. Szegedy, "Batch normalization : Accelerating deep network training by reducing internal covariate shift," in *ICML*, 2015. 5

[33] G. Hinton, N. Srivastava, A. Krizhevsky, I. Sutskever, and R. Salakhutdinov, "Improving neural networks by preventing co-adaptation of feature detectors," *arxiv :1207.0580*, 2012. 5